



## On the influence of stopping power formulations in the generation of fluorescence light at the shower axis

M. S. A. B. LEÃO<sup>1,\*</sup>, M. A. LEIGUI DE OLIVEIRA<sup>1</sup> AND C. J. TODERO PEIXOTO<sup>1</sup>

<sup>1</sup> Centro de Ciências Naturais e Humanas,

Universidade Federal do ABC,

09210-170, Santo André, SP, Brazil

\*milton.leao@ufabc.edu.br

DOI: 10.7529/ICRC2011/V02/1051

**Abstract:** The measurement of the fluorescence radiation in the atmosphere, induced by fast ionizing particles from ultra-high energy cosmic ray showers, is an important branch of research that has been opened up since the operation of the first fluorescence telescopes. The charged particles from the showers' electromagnetic component deposit part of their energy by the ionization and excitation of air molecules. These molecules, upon returning to their ground state, produce fluorescence light in the near-ultraviolet spectrum which can be detected as a track along the line of the showers' longitudinal development.

In this work, we present a detailed study on the energy deposit of electromagnetic particles in several atmospheric layers up to 35 km in altitude, taking into account parameterizations for density, temperature and composition of each layer and test different formulations for the energy deposit. Then, we use parameterizations for fluorescence yield to generate the total number of photons in the shower axis as a function of the slant depth.

**Keywords:** Stopping Power, Fluorescence Yield, Extensive Air Showers.

## 1 Introduction

High energy cosmic rays interacting in the Earth's atmosphere generate fluorescence light after the excitation of nitrogen molecules by air showers particles — mainly electrons and positrons with MeV energies. Telescopes have been assembled [1] [2] [3] and successfully used to measure the showers' longitudinal profile and reconstruct the properties of primaries exceeding  $10^{17}$  eV.

Based on the assumptions that the Fluorescence Yield (FY) of electrons in air is caused by de-excitation due to fluorescence emissions and non-radiative collisions, Bunner [4] suggested that the FY should be proportional to the energy deposit, or stopping power ( $dE/dx$ ), and parameterized by:

$$FY(K_e, \rho, T, \lambda) \propto \frac{dE}{dx}(K_e) \times \frac{\rho}{1 + \rho B \sqrt{T}} \quad (1)$$

where  $K_e$  is the electron kinetic energy,  $\rho$  is the air density,  $T$  is the air temperature and  $B$  is a constant. Moreover, one has to consider the wavelength in which the emission takes place since it occurs in peaks within some bandwidths in the interval of interest, i.e.  $300 < \lambda < 400$  nm.

Several experiments have been done for the measurements of these emissions, a review can be found in [5]. Kakimoto *et al.* [6] and Nagano *et al.* [7] measured the FY in air, induced by electrons emitted from a  $\beta$ -decay source ( $^{90}\text{Sr}$ ).

They extended Bunner's relation using two terms for the FY parameterization:

$$FY(K_e, \rho, T, \lambda) = \left\{ \frac{dE}{dx}(K_e) / \frac{dE}{dx}(K_e^{ref}) \right\} \times \left\{ \frac{\rho A_1}{1 + \rho B_1 \sqrt{T}} + \frac{\rho A_2}{1 + \rho B_2 \sqrt{T}} \right\} \quad (2)$$

where  $K_e^{ref}$  is the electron kinetic energy in the minimum energy deposit, used as a reference value, and  $A_1$ ,  $A_2$ ,  $B_1$  and  $B_2$  are constants whose experimental results are given in Table 1.

The energy deposit can be calculated using Bethe [8] and Bloch [9] formulas and their corrections. For electrons, one can express it as [10]:

$$-\frac{dE}{dx} [MeV \text{ cm}^2/g] = 0.1535 \rho \frac{Z}{A} \frac{1}{\beta^2} \times \left\{ \ln \frac{K_e^2 (K_e + 2)}{2(I/m_e c^2)^2} + F(K_e) - \delta - 2 \frac{C}{Z} \right\} \quad (3)$$

where  $\rho$  is the density,  $Z$  is the atomic number and  $A$  is the mass number of the absorbing medium;  $\beta = v/c$  is the ratio of the electron speed to the light speed and  $K_e$  the electron kinetic energy (in units of  $m_e c^2$ );  $I$  is the mean excitation potential,  $F(K_e)$  is a function whose form depends

| Parameter                                | Kakimoto <i>et al.</i> | Nagano <i>et al.</i> |
|--|------------------------|----------------------|
| $A_1 [m^2 kg^{-1}]$                      | $89.0 \pm 1.7$         | $147.4 \pm 4.3$      |
| $A_2 [m^2 kg^{-1}]$                      | $55.0 \pm 2.2$         | $69.8 \pm 12.2$      |
| $B_1 [m^3 kg^{-1} K^{-1/2}]$             | $1.85 \pm 0.04$        | $2.40 \pm 0.18$      |
| $B_2 [m^3 kg^{-1} K^{-1/2}]$             | $6.50 \pm 0.33$        | $20.1 \pm 6.9$       |
| $K_e^{ref} [MeV]$                        | 1.4                    | 0.85                 |
| $\frac{dE}{dx} (K_e^{ref}) [MeV g/cm^2]$ | 1.65                   | 1.67                 |

Table 1: Parameters of the equation 2, obtained experimentally by Kakimoto *et al.* [6] and Nagano *et al.* [7].

whether the incident particle is an electron or a positron,  $\delta$  is the density correction — due to the polarization of the atoms in the electrons' path — and  $C/Z$  is the shell correction.

Since the energy deposit in equation 3 is dependent on the medium density, to calculate the number of fluorescence photons, one must take into account the several air densities in each considered atmospheric depth. In figure 1, we present the energy deposit for electrons in air at several atmospheric layers, from the sea level up to 35 km in altitude, following standard density parameterizations.

## 2 Monte Carlo calculations of the energy loss

In order to compare the results of figure 1, we used other two formulations for the stopping power, both given by simulations: the software ESTAR [11] from NIST<sup>1</sup> and PEGS [12], the preprocessor for EGS<sup>2</sup>. These codes are widely used to simulate and generate data to electromagnetic interactions in material media. They apply the theory of Bethe and Bloch with density corrections evaluated according to Sternheimer [13].

In figure 2 one can find the comparison of the different formulations for  $dE/dx$ , as given by the theory (equation 3), NIST and PEGS. These results were obtained for dry air, at sea level with  $P = 1$  atm,  $T = 288$  K and  $\rho = 1.2$  kg/m<sup>3</sup>.

At the minimum ionization energy, the mean energy loss is 1.505, 1.661 and 1.054 MeV cm<sup>2</sup>/g, respectively, for equation 3, NIST and PEGS, which gives a discrepancy of about 58% between the results given by NIST and PEGS, where the result obtained by NIST is 10% higher and the one by PEGS is 30% lower than the theoretical.

## 3 Number of photons at the shower axis

The amount of fluorescence light produced near the shower axis is proportional to the energy deposited by electrons (and positrons) stopping in air. To evaluate the impact of the stopping power formulations on the generation of fluorescence light in air showers, we simulated, with CORSIKA [14], showers of seven fixed primary energies:  $10^{17}$ ,  $10^{17.5}$ ,  $10^{18}$ ,  $10^{18.5}$ ,  $10^{19}$ ,  $10^{19.5}$  and  $10^{20}$  eV. The primaries were chosen to be proton and iron and the zenith

angles were sorted between  $0^\circ$  and  $60^\circ$ . It has been simulated  $10^3$  events for each energy and composition.

The longitudinal development of the showers has been divided in layers of 5 g/cm<sup>2</sup>. Thus, for each layer, we read from CORSIKA the number and the energy of electrons and positrons and calculated the energy loss, according to the studied formulations. Finally, we applied Nagano *et al.* parameterization for the fluorescence yield, using standard profiles for the atmospheric density, pressure and temperature. We also supposed that 1% of the deposited energy is converted into fluorescence light.

Our results are shown in figures 3 and 4 for some selected energies. The lines' widths are given by one mean standard deviation at each atmospheric layer. As one can see, the values for the number of photons are varying in the same way as the stopping powers, namely, with a discrepancy of about 58% between NIST and PEGS results, where NIST is 10% higher and PEGS is 30% lower than the number given by theoretical energy loss.

## 4 Conclusions

We studied the changes in the number of photons produced at the shower axis by simulations, using different formulations for the energy deposit of electrons stopping in air at several atmospheric levels. The amount of photons has changed proportionally to the values of the stopping powers, as expected. Even though the energy deposit calculations, using Bethe and Bloch theory, must be taken as a limiting case and a more extensive simulation must be made, our results have shown an important influence of these formulations on the simulations. Therefore, the reconstruction chain of extensive air showers, if based on the energy deposit, are affected by the stopping power formulation used to predict the number of fluorescence photons.

## 5 Acknowledgments

We thank FAPESP (Fundação de Amparo à Pesquisa do Estado de São Paulo) by the financial support to this work and CENAPAD (Centro Nacional de Processamento de Alto Desempenho), where the simulations have been performed.

1. National Institute of Standards and Technology
2. Electron-Gamma-Shower

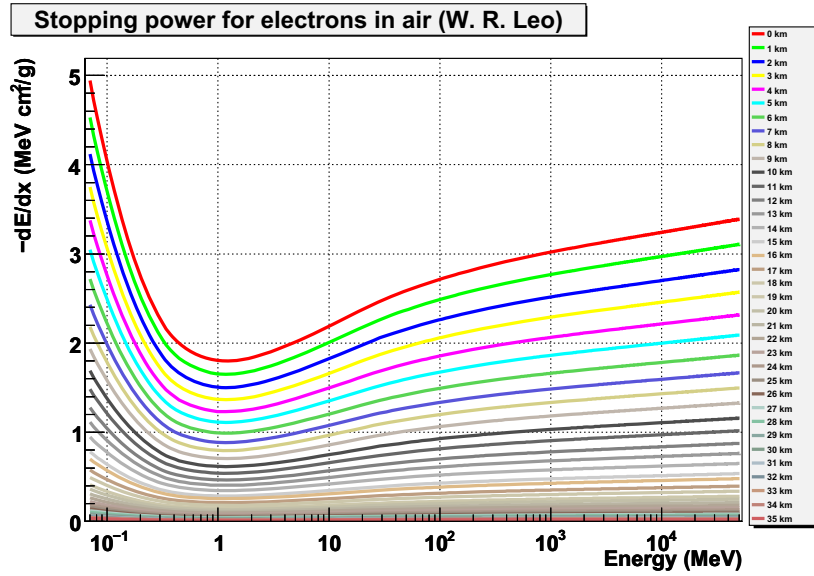


Figure 1: Energy deposit of electrons in air at each atmospheric level, according to equation 3.

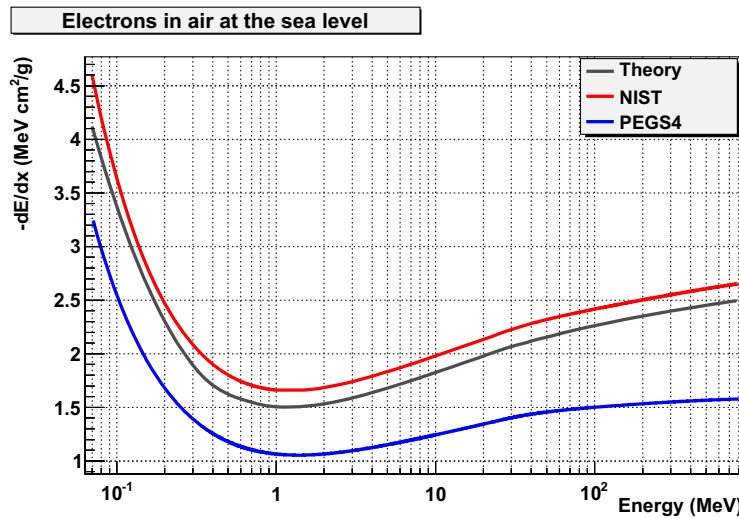


Figure 2: Comparison of the formulations for the energy deposit of electrons in air at the sea level.

**References**

[1] R. M. Baltrusaitis *et al.*, Nucl. Instr. and Meth. in Phys. Res., 1985, **A240**: 410.  
 [2] T. Abu-Zayyad *et al.*, Nucl. Instr. and Meth. in Phys. Res., 2000, **A450**: 253.  
 [3] J. Abraham *et al.*, Nucl. Instr. and Meth. in Phys. Res., 2004, **A523**: 50.  
 [4] A. N. Bunner: 1967, Cosmic Ray Detection by Atmospheric Fluorescence, PhD Thesis, Cornell University.  
 [5] F. Arqueros *et al.*, Proc. of the 5th Fluorescence Workshop, Madrid, Nucl. Instr. and Meth. in Phys. Res., 2008, **A597**: 1.  
 [6] K. Kakimoto *et al.*, Nucl. Instr. and Meth. in Phys. Res., 1996, **A372**: 527.  
 [7] M. Nagano *et al.*, Astrop. Phys., 2004, **22**: 235.  
 [8] H. Bethe, Ann. Phys., 1930, **5**: 325.  
 [9] F. Bloch, Z. Phys., 1933, **81**: 363.  
 [10] W. R. Leo: 1994, Techniques for Nuclear and Particle Physics Experiments, Springer-Verlog.  
 [11] <http://physics.nist.gov/PhysRefData/Star/Text/ESTAR.html>  
 [12] H. Hirayama *et al.*, PEGS User Manual SLAC-R-730/KEK-2005-8, Appendix C.  
 [13] R.M. Sternheimer, M.J. Berger and S. M. Seltzer, Atomic Nucl. Data Tables **30**, 261 (1984)  
 [14] D. Heck *et al.*, Report KfK 6019, Forschungszentrum Karlsruhe (1998).

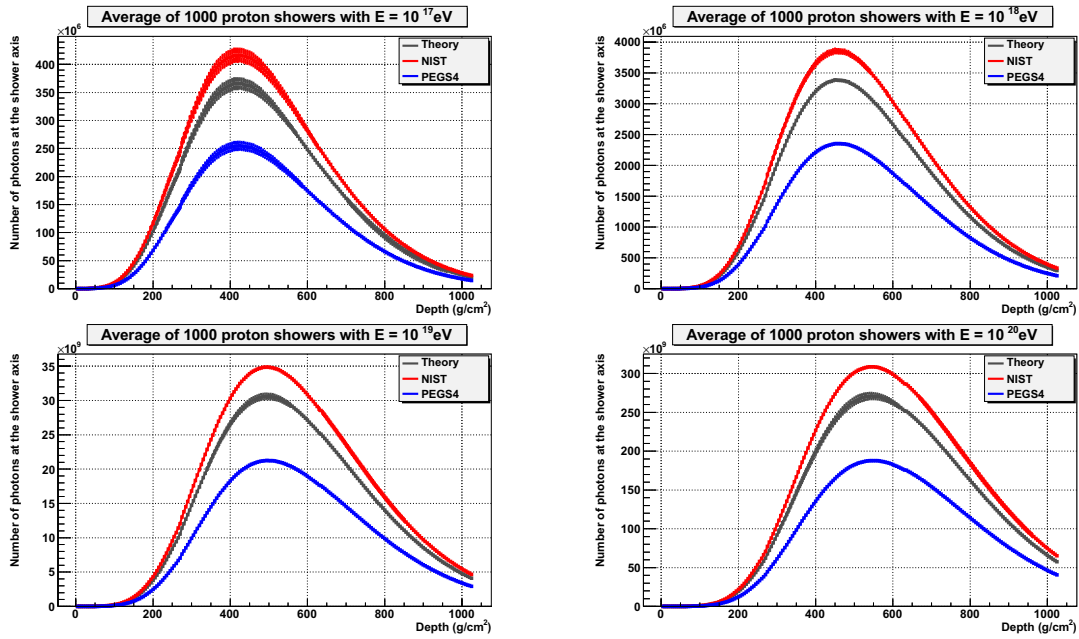


Figure 3: Average number of fluorescence photons at the shower axis for  $10^3$  proton-induced showers.

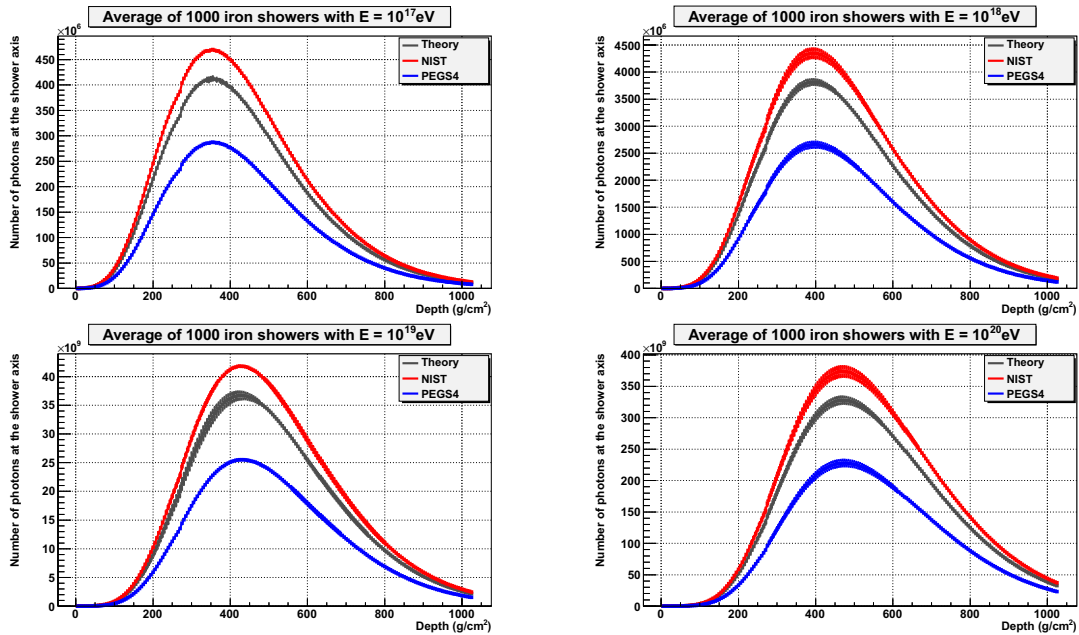


Figure 4: Average number of fluorescence photons at the shower axis for  $10^3$  iron-induced showers.